SCIENCE CHINA
Information Sciences

• RESEARCH PAPER •

September 2023, Vol. 66 190202:1–190202:14
https://doi.org/10.1007/s11432-022-3747-2

Special Topic: Control, Optimization, and Learning for Networked Systems

Sampled-data bipartite containment control over a network of wave equations

Yining CHEN[1,2], Zhiqiang ZUO[2*] & Yijing WANG[2]

[1]School of Artificial Intelligence, Tiangong University, Tianjin 300387, China;
[2]Tianjin Key Laboratory of Process Measurement and Control, School of Electrical and Information Engineering, Tianjin University, Tianjin 300072, China

Received 11 July 2022/Revised 1 November 2022/Accepted 14 March 2023/Published online 23 August 2023

Abstract This paper studies the bipartite containment control problem for a network of wave equations. A distributed sampled-data control protocol is proposed such that the follower states converge to a convex hull spanned by the leader trajectories and their opposites. A criterion for bipartite containment control is derived by applying the constructed Lyapunov-Krasovskii functional. The well-posedness of the closed-loop system is verified using the semigroup and induction methods. Furthermore, the effectiveness of the theoretical results is demonstrated through numerical examples.

Keywords bipartite containment control, sampled-data control, multi-agent system, partial differential equation

Citation Chen Y N, Zuo Z Q, Wang Y J. Sampled-data bipartite containment control over a network of wave equations. Sci China Inf Sci, 2023, 66(9): 190202, https://doi.org/10.1007/s11432-022-3747-2

1 Introduction

Recent decades have witnessed increasing research interest in cooperative control for multi-agent systems (MASs), primarily due to its numerous advantages such as cost reduction, efficiency, robustness, and wide applications ranging from engineering to social sciences [1–4]. In the case of multiple leaders, containment control aims to steer all the follower states into a convex hull spanned by the leader trajectories [5, 6]. Additionally, it has provided a general method for applications such as multi-robot obstacle avoiding and biological swarming networks [7–9], among several others. A common trait shared by these studies involves the exclusive incorporation of cooperative interactions. Moreover, the (weighted) adjacency matrix characterizing the communication topology among individuals contains only non-negative elements. In the real world, however, the coexistence of cooperative and antagonistic interactions must also be considered. Here, a signed graph is used, which allows for both positive and negative adjacency weights [10]. This is referred to as the bipartite containment control when related to a structurally balanced signed graph [11], in contrast to the traditional containment control formulation.

Extensive engineering applications, including attitude tracking for multiple flexible spacecraft and cooperative control for flexible manipulators [12, 13], have led to an increasing interest in the cooperative control of MASs based on partial differential equations (PDEs) networks. The consensus problem for networked parabolic PDEs under the undirected communication graph was solved in [14]. Boundary control protocols were proposed in [15] to address the consensus issue for networked parabolic PDEs. Refs. [16,17] considered the cooperative output regulation issue for parabolic agents. Recent advances also include the leader-follower synchronization over networks of wave equations [18, 19]. Bipartite consensus for networked wave equations was studied when there exist competitive interactions [20, 21]. The scaled consensus problem was further discussed in [22]. A general class of distributed parameter agents was investigated using the abstract setting in [23, 24]. Additionally, Refs. [25–27] studied the networked control of finite-dimensional MASs by employing the PDE theory. Unlike the aforementioned references,

* Corresponding author (email: zqzuo@tju.edu.cn)

© Science China Press 2023

we primarily focus on the topic of containment control subject to antagonistic interactions from the PDE perspective. This topic is both involving and challenging because of the complex dynamic phenomena and abstruse theory involved. To the best of the authors' knowledge, few results on this subject are available in the literature.

One of the downsides uncovered in existing studies is the strong dependence of continuous input signals on space or time. Sampled-data control that updates the signals in a discrete-time manner has been widely implemented in some modern control systems, particularly in the finite-dimensional frameworks [28–30]. However, on the infinite-dimensional counterpart, little work on sampled-data control has been done owing to technical difficulties. The main contributions to these results have focused on parabolic PDE systems and sampled-data feedback controllers via matrix inequalities [31,32] and the backstepping approach [33]. Until recently, tangible progress has been made for hyperbolic systems [34,35]. In the context of abstract infinite-dimensional systems, semigroup technology is often used for periodic sampling [36, 37]. It is worthwhile to point out that the concept of sampled-data control has not yet been studied for cooperative PDE-modeled MASs. The reasons can be summarized in three points: (1) An intuitive difficulty lies in the PDE. Compared with traditional MASs, the dynamic systems described by PDEs may contain an infinite number of eigenvalues [38], posing challenges to the problem at hand. (2) Another problem arises due to the directed graph represented via an asymmetric Laplacian matrix. In particular, it does not satisfy the invertible property, leading to some difficulties in analysis and synthesis. Furthermore, the eigenvalues of the Laplacian matrix could be complex, resulting in a massive computational burden. (3) Many universal techniques typically employed in continuous-time systems become invalid for the discrete-time case. New tools are expected to address technical barriers in controller design and analysis caused by discrete inputs.

Consequently, we extend the concept of bipartite containment control to a network of wave equations in the sequel. Unlike most existing studies, discrete state measurements sampled in both space and time are used to construct the distributed control protocol with variable and bounded sampling intervals. It should be noted that the extension is nontrivial and the introduced discontinuous input signals always result in challenging analysis. To address this issue, a suitable Lyapunov-Krasovskii functional is proposed to ensure the bipartite containment control of the underlying system. Subsequently, sufficient conditions that ensure the goal and convergence rate are obtained simultaneously. Moreover, well-posedness is guaranteed by the semigroup and induction methods. The contributions of this study are threefold:

(i) Competitive interactions are considered, and the bipartite containment control problem as well as its well-posedness is solved within the PDE framework, thus extending the previous bipartite containment control in a finite-dimensional setting.

(ii) A distributed sampled-data control scheme is provided to ensure bipartite containment control. This strategy can operate feasibly and fulfill the digital signal requirement, whereas some continuous inputs in [14, 15, 18, 19] rely on uninterrupted updates.

(iii) The directed communication topology used in this paper relaxes the undirected and connected constraints in [15, 18]. Therefore, the derived results will be used in more general situations.

The remainder of this paper is organized as follows. Section 2 presents the studied problem and discusses some of the preliminaries. The bipartite containment control is achieved using the proposed distributed sampled-data protocol in Section 3. Moreover, the well-posedness analysis of the closed-loop system is provided in Section 4. Several numerical simulations are presented in Section 5 to verify the effectiveness of the theoretical results. Finally, Section 6 concludes this paper.

2 Preliminaries and problem description

2.1 Notations and useful lemma

Symbols $\mathbf{1}_N = (1, 1, \ldots, 1)^\top$ and $\mathbf{0}_N = (0, 0, \ldots, 0)^\top$ refer to the all-ones and all-zeros vectors, respectively. $\mathbb{R}^N$ stands for the N-dimensional real vector space. Space $\mathbb{R}^{N\times N}$ includes all $N \times N$-dimensional matrices with real elements.

The following inequality will be helpful.

Lemma 1 ([39], Halanay's inequality). For $0 < \alpha_1 < \alpha_0$ and an absolutely continuous function $V : [t_0 - T, \infty) \to [0, \infty)$, if

$$\dot{V}(t) + 2\alpha_0 V(t) - 2\alpha_1 \sup_{-T \leqslant \theta \leqslant 0} V(t+\theta) \leqslant 0, \quad t \geqslant t_0,$$

then

$$V(t) \leqslant \mathrm{e}^{-2\alpha(t-t_0)} \sup_{-T\leqslant\theta\leqslant 0} V(t_0+\theta), \quad t \geqslant t_0,$$

where $\alpha > 0$ is the unique positive solution of $\alpha = \alpha_0 - \alpha_1 \mathrm{e}^{2\alpha T}$.

2.2 Problem statement

Consider a collection of N followers and M leaders, with notations $v^f(x,t) \triangleq (v_1(x,t),\ldots,v_N(x,t))^\top \in \mathbb{R}^N$ and $v^l(x,t) \triangleq (v_{N+1}(x,t),\ldots,v_{N+M}(x,t))^\top \in \mathbb{R}^M$ reflecting the transverse deflections of the followers and leaders at position $x \in (0,1)$ and time $t \in [0,\infty)$, respectively. Then, the dynamics of networked PDEs can be given by

$$\begin{cases} v_{tt}(x,t) = v_{xx}(x,t) + U(x,t), \\ v(0,t) = \mathbf{0}_{N+M}, \\ v_x(1,t) = -v_t(1,t), \\ v(x,t_0) = v_0(x), \quad v_t(x,t_0) = v_1(x), \end{cases} \tag{1}$$

where $v(x,t) \triangleq (v^{f\top}(x,t), v^{l\top}(x,t))^\top \in \mathbb{R}^{N+M}$. Without loss of generality, v_t (v_x) and v_{tt} (v_{xx}) represent the abbreviations for the first and second order derivatives of v with respect to time t (position x), respectively. $v_0(x)$ and $v_1(x)$ are the initial deflection and velocity of $N+M$ PDE agents. Let $U(x,t) \triangleq (u^\top(x,t), \mathbf{0}_M^\top)^\top$, in which $u(x,t) \triangleq (u_1(x,t),\ldots,u_N(x,t))^\top \in \mathbb{R}^N$ corresponds to the control protocol acting on the followers.

In this study, the interaction among PDE agents is described by a (weighted) signed digraph $\mathcal{G} \triangleq \{\mathcal{V},\mathcal{E}\}$, where $\mathcal{V} \triangleq \{1,2,\ldots,N+M\}$ is the set of agents and $\mathcal{E} \subseteq \mathcal{V}\times\mathcal{V} = \{(i,j) : i,j \in \mathcal{V}\}$ refers to the edge set such that (i,j) is a directed edge from j to i. The elements of adjacency matrix $\mathcal{A} \triangleq (a_{ij})_{(N+M)\times(N+M)}$ denotes signed weights: $a_{ij} > 0$ ($a_{ij} < 0$) if there exists friendly (adversarial) interaction between the two agents. Otherwise, $a_{ij} = 0$. Furthermore, there is no self-loop in the graph, i.e., $a_{ii} = 0$. The signed digraph is digon sign-symmetric if $a_{ij}a_{ji} \geqslant 0$ for any $i,j \in \mathcal{V}$. Let the degree matrix $\boldsymbol{D} \triangleq \mathrm{diag}\{\boldsymbol{D}_1,\ldots,\boldsymbol{D}_{N+M}\}$ in which $\boldsymbol{D}_i = \sum_{j=1}^{N+M} |a_{ij}|$. Then, in the case of no information exchange among the leaders, the corresponding Laplacian matrix can be represented by

$$\mathcal{L} \triangleq \boldsymbol{D} - \mathcal{A} = \begin{pmatrix} \mathcal{L}_1 & \mathcal{L}_2 \\ 0_{M\times N} & 0_{M\times M} \end{pmatrix},$$

where $\mathcal{L}_1 \triangleq \mathcal{L}_f + \mathrm{diag}\{\sum_{j=N+1}^{N+M} |a_{1j}|,\ldots,\sum_{j=N+1}^{N+M} |a_{Nj}|\} \in \mathbb{R}^{N\times N}$, $\mathcal{L}_2 \in \mathbb{R}^{N\times M}$, $0_{M\times N}$ and $0_{M\times M}$ are real matrices with proper dimensions. Additionally, $\mathcal{L}_f$ is the Laplacian matrix associated with the adjacency matrix of $\bar{\mathcal{G}} \triangleq \{\bar{\mathcal{V}},\bar{\mathcal{E}}\}$ which is composed of the followers set $\bar{\mathcal{V}} \triangleq \{1,2,\ldots,N\}$ and the edges set $\bar{\mathcal{E}} \subseteq \bar{\mathcal{V}}\times\bar{\mathcal{V}}$. The signed subgraph $\bar{\mathcal{G}}$ is structurally balanced if there is a bipartition $\{\bar{\mathcal{V}}_1,\bar{\mathcal{V}}_2\}$ such that $\bar{\mathcal{V}}_1 \cup \bar{\mathcal{V}}_2 = \bar{\mathcal{V}}$, $\bar{\mathcal{V}}_1 \cap \bar{\mathcal{V}}_2 = \emptyset$, and

(i) $a_{ij} \geqslant 0$, $i,j \in \bar{\mathcal{V}}_p$, $p = 1,2$,

(ii) $a_{ij} \leqslant 0$, $i \in \bar{\mathcal{V}}_p$, and $j \in \bar{\mathcal{V}}_r$, $p \neq r$.

Otherwise, the subgraph $\bar{\mathcal{G}}$ is structurally unbalanced. Let $\sigma_i = 1$ for $i \in \bar{\mathcal{V}}_1$ and $\sigma_i = -1$ for $i \in \bar{\mathcal{V}}_2$. In addition, let $\mathcal{D} \triangleq \mathrm{diag}\{\sigma_1,\sigma_2,\ldots,\sigma_N\}$.

Our goal is to provide an appropriate distributed protocol such that the PDE multi-agent system (1) achieves bipartite containment control. In such a case, the follower states of different subgroups converge to a convex hull spanned by the leader orbits and their opposite trajectories. This case necessitates the following assumptions.

Assumption 1. For each follower, there must be at least one leader transmitting information to the follower.

Assumption 2. For subgraph $\bar{\mathcal{G}}$, the communication topology is structurally balanced.

In terms of Assumptions 1 and 2, the following lemmas can be derived.

Lemma 2 ([7,11])**.** Matrix $\mathcal{L}_1$ is nonsingular, and all its eigenvalues have positive real parts.

Lemma 3 ([7])**.** $\mathcal{D}\mathcal{L}_1\mathcal{D}$ is a nonsingular M-matrix. Additionally, each element of matrix $-\mathcal{D}\mathcal{L}_1^{-1}\mathcal{D}\mathcal{L}_2$ is non-negative, with all row sums being 1. Therefore, $-\mathcal{D}\mathcal{L}_1^{-1}\mathcal{D}\mathcal{L}_2 Y$ is a convex hull spanned by multiple leader states with $Y \triangleq (Y_1,Y_2,\ldots,Y_M)^\top$.

We are now in the position to formulate the definition of bipartite containment control in terms of Lemma 3.

Definition 1 (Bipartite containment control)**.** For system (1), if

$$\lim_{t\to\infty}\left\|\mathcal{D}v^f(\cdot,t)+\mathcal{D}\mathcal{L}_1^{-1}\mathcal{D}\mathcal{L}_2v^l(\cdot,t)\right\|_{L^2}=0,$$

we say that it achieves bipartite containment control in the sense of L^2.

Remark 1. Note that the traditional graph associated with the non-negative adjacency weight matrices can be regarded as a special case of a structurally balanced signed one. In this case, the MASs achieve containment control.

3 Protocol design and bipartite containment control

In this section, a control protocol is developed using measurements obtained from sampled data in space and time to ensure bipartite containment control.

Specifically, the sampling time instants are

$$0=t_0<t_1<\cdots<t_k,\quad \lim_{k\to\infty}t_k=\infty.$$

The space segment $[0,1]$ is divided into m sampling intervals by $m+1$ points $0=x_0<x_1<\cdots<x_m=1$. Through the sensors placed at the center point $\bar{x}_j=\frac{x_j+x_{j+1}}{2}$ of each space interval $[x_j,x_{j+1}]$, output information $v(\bar{x}_j,t_k)$, $j=0,1,\ldots,m-1$, $k=0,1,2,\ldots$, is transmitted. Here, the sampling intervals in terms of time and space are bounded by positive constants T and X, that is,

$$0\ <\ t_{k+1}-t_k\leqslant T,\quad x_{j+1}-x_j\leqslant X.$$

We propose the distributed protocol based on the sampling information as follows:

$$U(x,t)=\begin{pmatrix}-\kappa\sum_{j=0}^{m-1}\chi_j(x)\mathcal{L}_1\epsilon(\bar{x}_j,t_k)\\ \mathbf{0}_M\end{pmatrix},\tag{2}$$

where $\kappa>0$ is the control gain and

$$\epsilon(x,t)\triangleq\mathcal{D}v^f(x,t)+\mathcal{D}\mathcal{L}_1^{-1}\mathcal{D}\mathcal{L}_2v^l(x,t)\tag{3}$$

is the error vector. Obviously, the error $\epsilon(x,t)$ satisfies

$$\begin{cases}\epsilon_{tt}(x,t)=\epsilon_{xx}(x,t)-\kappa\sum_{j=0}^{m-1}\chi_j(x)\mathcal{D}\mathcal{L}_1\epsilon(\bar{x}_j,t_k),\\ \epsilon(0,t)=\mathbf{0}_N,\quad \epsilon_x(1,t)=-\epsilon_t(1,t),\\ \epsilon(x,0)=\epsilon_0(x),\quad \epsilon_t(x,0)=\epsilon_1(x).\end{cases}\tag{4}$$

Note that the multi-agent system (1) achieves bipartite containment control if the error system (4) is asymptotically stable. For this purpose, let us introduce new variables

$$\begin{aligned}R(x,t)&\triangleq\epsilon_t(x,t)-\epsilon_x(x,t),\\ Q(x,t)&\triangleq\epsilon_t(x,t)+\epsilon_x(x,t).\end{aligned}\tag{5}$$

Following [40], system (4) can be transformed into a characteristic form in the Riemann coordinates

$$\begin{cases}R_t(x,t)=-R_x(x,t)-\kappa\mathcal{D}\mathcal{L}_1\epsilon(x,t)+\sigma,\\ Q_t(x,t)=Q_x(x,t)-\kappa\mathcal{D}\mathcal{L}_1\epsilon(x,t)+\sigma,\\ R(0,t)=-Q(0,t),\quad Q(1,t)=\mathbf{0}_N,\end{cases}\tag{6}$$

in which

$$\sigma=\kappa\sum_{j=0}^{m-1}\chi_j(x)\mathcal{D}\mathcal{L}_1\left[(t-t_k)w+\int_{\bar{x}_j}^{x}\epsilon_\xi(\xi,t_k)\mathrm{d}\xi\right],$$

$$w = \frac{1}{t - t_k} \int_{t_k}^{t} \epsilon_s(x, s)\mathrm{d}s. \tag{7}$$

The following Lyapunov-Krasovskii functional is constructed to ensure that system (6), equivalently the error system (4), is asymptotically stable:

$$V(t) = V_q(t) + V_\gamma(t), \quad t \in [t_k, t_{k+1}), \tag{8}$$

where

$$\begin{aligned} V_q(t) &= \int_0^1 q_1 \mathrm{e}^{-\mu x} R^\top(x,t)R(x,t) + q_2 \mathrm{e}^{\mu x} Q^\top(x,t)Q(x,t)\mathrm{d}x, \\ V_\gamma(t) &= \gamma \int_0^1 \left[(t_{k+1} - t)\int_{t_k}^{t} \mathrm{e}^{2\alpha_0(s-t)} \epsilon_s^\top(\xi,s)\epsilon_s(\xi,s)\mathrm{d}s\right]\mathrm{d}\xi, \end{aligned}$$

with positive parameters q_1, q_2, μ, γ, and α_0.

The following theorem is derived as the main result of this section using Halanay's inequality.

Theorem 1. Suppose that Assumptions 1 and 2 hold true. Subject to the conditions $X > 0$ and $T > 0$, if the parameters in Lyapunov-Krasovskii functional (8) satisfy

$$\begin{cases} 0 \leqslant q_2 - q_1, \\ q_1 + q_2 \leqslant 1, \\ 0 < \alpha_1 < \alpha_0 < \frac{1}{2}\mu, \end{cases} \tag{9}$$

and

$$\gamma < \frac{2(\mu - 2\alpha_0)}{T} \min\{q_1 \mathrm{e}^{-2\mu},\ q_2 \mathrm{e}^{-\mu}\}, \tag{10}$$

then one can choose

$$0 < \tau_1 \leqslant 4\alpha_1 \min\{q_1 \mathrm{e}^{-\mu},\ q_2\} \tag{11}$$

and

$$\begin{aligned} 0 < \kappa < \min\Bigg\{ &\frac{(\mu - 2\alpha_0)q_1 - \frac{\gamma}{2}(T-s)\mathrm{e}^{2\mu}}{2q_1 + q_1 s + \frac{2}{\pi^2}\lambda_{\max}(\mathcal{L}_1^\top \mathcal{L}_1)\mathrm{e}^{2\mu}},\ \frac{(\mu - 2\alpha_0)q_2 \mathrm{e}^{-\mu} - \frac{\gamma}{2}(T-s)}{2q_2 + q_2 s + \frac{2}{\pi^2}\lambda_{\max}(\mathcal{L}_1^\top \mathcal{L}_1)}, \\ &\frac{\tau_1 \pi^2}{X^2(q_1+q_2)\lambda_{\max}(\mathcal{L}_1^\top \mathcal{L}_1)},\ \frac{\gamma \mathrm{e}^{-2\alpha_0 T}}{(q_1+q_2)\lambda_{\max}(\mathcal{L}_1^\top \mathcal{L}_1)}\Bigg\}, \qquad s = 0, T, \end{aligned} \tag{12}$$

such that the PDE multi-agent system (1) with control protocol (2) achieves bipartite containment control.

Proof. Differentiating $V_q(t)$ along the trajectory of error system (6) and integrating by parts, one obtains

$$\begin{aligned} \dot{V}_q(t) &= 2\int_0^1 q_1 \mathrm{e}^{-\mu x} R^\top(x,t)R_t(x,t)\mathrm{d}x + 2\int_0^1 q_2 \mathrm{e}^{\mu x} Q^\top(x,t)Q_t(x,t)\mathrm{d}x \\ &= 2\int_0^1 \left[q_1 \mathrm{e}^{-\mu x} R^\top(x,t) + q_2 \mathrm{e}^{\mu x} Q^\top(x,t)\right]\left[-\kappa \mathcal{D}\mathcal{L}_1 \epsilon(x,t) + \sigma\right]\mathrm{d}x \\ &\quad - 2\int_0^1 q_1 \mathrm{e}^{-\mu x} R^\top(x,t)R_x(x,t)\mathrm{d}x + 2\int_0^1 q_2 \mathrm{e}^{\mu x} Q^\top(x,t)Q_x(x,t)\mathrm{d}x \\ &= -\int_0^1 q_1 \mathrm{e}^{-\mu x} \frac{\partial}{\partial x}(R^\top R)dx + \int_0^1 q_2 \mathrm{e}^{\mu x} \frac{\partial}{\partial x}(Q^\top Q)\mathrm{d}x \\ &\quad + 2\int_0^1 \left[q_1 \mathrm{e}^{-\mu x} R^\top(x,t) + q_2 \mathrm{e}^{\mu x} Q^\top(x,t)\right]\left[-\kappa \mathcal{D}\mathcal{L}_1 \epsilon(x,t) + \sigma\right]\mathrm{d}x \\ &= -q_1 \mathrm{e}^{-\mu} R^\top(1,t)R(1,t) + q_1 R^\top(0,t)R(0,t) + q_2 \mathrm{e}^{\mu} Q^\top(1,t)Q(1,t) - q_2 Q^\top(0,t)Q(0,t) \end{aligned}$$

$$- \mu \int_0^1 q_1 \mathrm{e}^{-\mu x} R^\top(x,t) R(x,t) \mathrm{d}x - \mu \int_0^1 q_2 \mathrm{e}^{\mu x} Q^\top(x,t) Q(x,t) \mathrm{d}x$$
$$+ 2 \int_0^1 \big[q_1 \mathrm{e}^{-\mu x} R^\top(x,t) + q_2 \mathrm{e}^{\mu x} Q^\top(x,t)\big]\big[-\kappa \mathcal{D}\mathcal{L}_1 \epsilon(x,t) + \sigma\big] \mathrm{d}x.$$

Therefore, by substituting the boundary conditions, it is evident that

$$\begin{aligned}\dot{V}_q(t) = & -q_1 \mathrm{e}^{-\mu} R^\top(1,t) R(1,t) - (q_2 - q_1) R^\top(0,t) R(0,t) - \mu V_q(t) \\ & + 2 \int_0^1 \big[q_1 \mathrm{e}^{-\mu x} R^\top(x,t) + q_2 \mathrm{e}^{\mu x} Q^\top(x,t)\big]\big[-\kappa \mathcal{D}\mathcal{L}_1 \epsilon(x,t) + \sigma\big] \mathrm{d}x.\end{aligned}$$

Analogously, by taking the derivative of $V_\gamma(t)$, one derives

$$\begin{aligned}&\dot{V}_\gamma(t) + 2\alpha_0 V_\gamma(t) \\ &\leqslant -\gamma \int_0^1 \left[\int_{t_k}^t \mathrm{e}^{2\alpha_0(s-t)} \epsilon_s^\top(\xi,s)\epsilon_s(\xi,s) \mathrm{d}s\right] \mathrm{d}\xi + \gamma(t_{k+1} - t) \int_0^1 \epsilon_t^\top(x,t) \epsilon_t(x,t) \mathrm{d}x.\end{aligned}$$

Combining the above inequalities, we arrive at

$$\begin{aligned}&\dot{V}(t) + 2\alpha_0 V(t) - 2\alpha_1 \sup_{-T \leqslant \theta \leqslant 0} V(t+\theta) \\ &\leqslant \dot{V}(t) + 2\alpha_0 V(t) \\ &\quad - 2\alpha_1 \int_0^1 q_1 \mathrm{e}^{-\mu x} R^\top(x,t_k) R(x,t_k) \mathrm{d}x - 2\alpha_1 \int_0^1 q_2 \mathrm{e}^{\mu x} Q^\top(x,t_k) Q(x,t_k) \mathrm{d}x \\ &\leqslant -q_1 \mathrm{e}^{-\mu} R^\top(1,t) R(1,t) - (q_2 - q_1) R^\top(0,t) R(0,t) - (\mu - 2\alpha_0) V_q(t) \\ &\quad + 2 \int_0^1 \big[q_1 \mathrm{e}^{-\mu x} R^\top(x,t) + q_2 \mathrm{e}^{\mu x} Q^\top(x,t)\big]\big[-\kappa \mathcal{D}\mathcal{L}_1 \epsilon(x,t) + \sigma\big] \mathrm{d}x \\ &\quad - \gamma \int_0^1 \left[\int_{t_k}^t \mathrm{e}^{2\alpha_0(s-t)} \epsilon_s^\top(\xi,s)\epsilon_s(\xi,s) \mathrm{d}s\right] \mathrm{d}\xi + \gamma(t_{k+1} - t) \int_0^1 \epsilon_t^\top(x,t) \epsilon_t(x,t) \mathrm{d}x \\ &\quad - 2\alpha_1 \int_0^1 q_1 \mathrm{e}^{-\mu x} R^\top(x,t_k) R(x,t_k) \mathrm{d}x - 2\alpha_1 \int_0^1 q_2 \mathrm{e}^{\mu x} Q^\top(x,t_k) Q(x,t_k) \mathrm{d}x. \end{aligned} \tag{13}$$

Applying Jensen's inequality, we have

$$\begin{aligned}&- \gamma \int_0^1 \left[\int_{t_k}^t \mathrm{e}^{2\alpha_0(s-t)} \epsilon_s^\top(\xi,s)\epsilon_s(\xi,s) \mathrm{d}s\right] \mathrm{d}\xi \\ &\quad \leqslant -\gamma \mathrm{e}^{-2\alpha_0 T} \int_0^1 \left[\int_{t_k}^t \epsilon_s^\top(\xi,s)\epsilon_s(\xi,s) \mathrm{d}s\right] \mathrm{d}\xi \\ &\quad \leqslant -\gamma \mathrm{e}^{-2\alpha_0 T} \int_0^1 \frac{1}{t - t_k} \left[\int_{t_k}^t \epsilon_s(\xi,s) \mathrm{d}s\right]^\top \left[\int_{t_k}^t \epsilon_s(\xi,s) \mathrm{d}s\right] \mathrm{d}\xi \\ &\quad = -\gamma \mathrm{e}^{-2\alpha_0 T}(t - t_k) \sum_{j=0}^{m-1} \int_{x_j}^{x_{j+1}} w^\top w \mathrm{d}x. \end{aligned} \tag{14}$$

In addition, according to the definitions of $R(x,t)$ and $Q(x,t)$ in (5), one gets

$$\begin{aligned}&\gamma(t_{k+1} - t) \int_0^1 \epsilon_t^\top(x,t) \epsilon_t(x,t) \mathrm{d}x \\ &\quad = \frac{\gamma}{4}(t_{k+1} - t) \sum_{j=0}^{m-1} \int_{x_j}^{x_{j+1}} \big[Q^\top(x,t) + R^\top(x,t)\big]\big[Q(x,t) + R(x,t)\big] \mathrm{d}x. \end{aligned} \tag{15}$$

Therefore, substitute (14) and (15) into (13) to obtain

$$\dot{V}(t) + 2\alpha_0 V(t) - 2\alpha_1 \sup_{-T \leqslant \theta \leqslant 0} V(t+\theta)$$

$$
\begin{aligned}
&\leqslant -q_1\mathrm{e}^{-\mu}R^\top(1,t)R(1,t)-(q_2-q_1)R^\top(0,t)R(0,t)\\
&-(\mu-2\alpha_0)\sum_{j=0}^{m-1}\int_{x_j}^{x_{j+1}}q_1\mathrm{e}^{-\mu x}R^\top(x,t)R(x,t)\mathrm{d}x-(\mu-2\alpha_0)\sum_{j=0}^{m-1}\int_{x_j}^{x_{j+1}}q_2\mathrm{e}^{\mu x}Q^\top(x,t)Q(x,t)\mathrm{d}x\\
&-2\kappa\sum_{j=0}^{m-1}\int_{x_j}^{x_{j+1}}q_1\mathrm{e}^{-\mu x}R^\top(x,t)\mathcal{D}\mathcal{L}_1\epsilon(x,t)\mathrm{d}x-2\kappa\sum_{j=0}^{m-1}\int_{x_j}^{x_{j+1}}q_2\mathrm{e}^{\mu x}Q^\top(x,t)\mathcal{D}\mathcal{L}_1\epsilon(x,t)\mathrm{d}x\\
&+2\kappa\sum_{j=0}^{m-1}\int_{x_j}^{x_{j+1}}\big[q_1\mathrm{e}^{-\mu x}R^\top(x,t)+q_2\mathrm{e}^{\mu x}Q^\top(x,t)\big]\mathcal{D}\mathcal{L}_1\left[(t-t_k)w+\int_{\bar{x}_j}^{x}\epsilon_\xi(\xi,t_k)\mathrm{d}\xi\right]\mathrm{d}x\\
&-\gamma\mathrm{e}^{-2\alpha_0T}(t-t_k)\sum_{j=0}^{m-1}\int_{x_j}^{x_{j+1}}w^\top w\mathrm{d}x\\
&+\frac{\gamma}{4}(t_{k+1}-t)\sum_{j=0}^{m-1}\int_{x_j}^{x_{j+1}}\big[Q^\top(x,t)+R^\top(x,t)\big]\big[Q(x,t)+R(x,t)\big]\mathrm{d}x\\
&-2\alpha_1\sum_{j=0}^{m-1}\int_{x_j}^{x_{j+1}}q_1\mathrm{e}^{-\mu x}R^\top(x,t_k)R(x,t_k)\mathrm{d}x-2\alpha_1\sum_{j=0}^{m-1}\int_{x_j}^{x_{j+1}}q_2\mathrm{e}^{\mu x}Q^\top(x,t_k)Q(x,t_k)\mathrm{d}x.
\end{aligned}\tag{16}
$$

Moreover, by resorting to Wirtinger's inequality in [41], it is revealed that

$$
\int_0^1\epsilon^\top(x,t)\mathcal{L}_1^\top\mathcal{L}_1\epsilon(x,t)\mathrm{d}x\leqslant\frac{\lambda_{\max}\big(\mathcal{L}_1^\top\mathcal{L}_1\big)}{\pi^2}\int_0^1\big[Q^\top(x,t)-R^\top(x,t)\big]\big[Q(x,t)-R(x,t)\big]\mathrm{d}x
$$

and

$$
\begin{aligned}
&\frac{1}{4}\int_{x_j}^{x_{j+1}}\big[\epsilon(x,t_k)-\epsilon(\bar{x}_j,t_k)\big]^\top\big[\epsilon(x,t_k)-\epsilon(\bar{x}_j,t_k)\big]\mathrm{d}x\\
&\quad=\frac{1}{4}\int_{x_j}^{\bar{x}_j}\big[\epsilon(x,t_k)-\epsilon(\bar{x}_j,t_k)\big]^\top\big[\epsilon(x,t_k)-\epsilon(\bar{x}_j,t_k)\big]\mathrm{d}x\\
&\qquad+\frac{1}{4}\int_{\bar{x}_j}^{x_{j+1}}\big[\epsilon(x,t_k)-\epsilon(\bar{x}_j,t_k)\big]^\top\big[\epsilon(x,t_k)-\epsilon(\bar{x}_j,t_k)\big]\mathrm{d}x\\
&\quad\leqslant\frac{X^2}{4\pi^2}\int_{x_j}^{\bar{x}_j}\epsilon_x^\top(x,t_k)\epsilon_x(x,t_k)\mathrm{d}x+\frac{X^2}{4\pi^2}\int_{\bar{x}_j}^{x_{j+1}}\epsilon_x^\top(x,t_k)\epsilon_x(x,t_k)\mathrm{d}x\\
&\quad=\frac{X^2}{4\pi^2}\int_{x_j}^{x_{j+1}}\epsilon_x^\top(x,t_k)\epsilon_x(x,t_k)\mathrm{d}x.
\end{aligned}
$$

Consequently, we have

$$
\begin{aligned}
&\frac{\kappa}{\pi^2}\sum_{j=0}^{m-1}\int_{x_j}^{x_{j+1}}\lambda_{\max}\big(\mathcal{L}_1^\top\mathcal{L}_1\big)s\big[Q^\top(x,t)-R^\top(x,t)\big]\big[Q(x,t)-R(x,t)\big]\mathrm{d}x\\
&\quad-\kappa\sum_{j=0}^{m-1}\int_{x_j}^{x_{j+1}}\epsilon^\top(x,t)\mathcal{L}_1^\top\mathcal{L}_1\epsilon(x,t)\mathrm{d}x\geqslant 0,
\end{aligned}\tag{17}
$$

and

$$
\begin{aligned}
&\frac{\tau_1}{4}\sum_{j=0}^{m-1}\int_{x_j}^{x_{j+1}}\big[Q(x,t_k)-R(x,t_k)\big]^\top\big[Q(x,t_k)-R(x,t_k)\big]\mathrm{d}x\\
&\quad-\tau_1\frac{\pi^2}{X^2}\sum_{j=0}^{m-1}\int_{x_j}^{x_{j+1}}\int_{\bar{x}_j}^{x}\epsilon_\xi^\top(\xi,t_k)\mathrm{d}\xi\int_{\bar{x}_j}^{x}\epsilon_\xi(\xi,t_k)\mathrm{d}\xi\mathrm{d}x\geqslant 0,
\end{aligned}\tag{18}
$$

where $\tau_1 > 0$. To address the positive terms in (16), we introduce the non-negative items (17) and (18) for (16) to obtain

$$\begin{aligned}
&\dot{V}(t) + 2\alpha_0 V(t) - 2\alpha_1 \sup_{-T\leqslant\theta\leqslant 0} V(t+\theta)\\
&\leqslant -q_1 \mathrm{e}^{-\mu} R^\top(1,t)R(1,t) - (q_2 - q_1)R^\top(0,t)R(0,t)\\
&\quad - (\mu - 2\alpha_0)\sum_{j=0}^{m-1}\int_{x_j}^{x_{j+1}} q_1 \mathrm{e}^{-\mu x} R^\top(x,t)R(x,t)\mathrm{d}x - (\mu - 2\alpha_0)\sum_{j=0}^{m-1}\int_{x_j}^{x_{j+1}} q_2 \mathrm{e}^{\mu x} Q^\top(x,t)Q(x,t)\mathrm{d}x\\
&\quad - 2\kappa\sum_{j=0}^{m-1}\int_{x_j}^{x_{j+1}} \big[q_1 \mathrm{e}^{-\mu x} R^\top(x,t) + q_2 \mathrm{e}^{\mu x} Q^\top(x,t)\big]\mathcal{D}\mathcal{L}_1 \epsilon(x,t)\mathrm{d}x - \gamma \mathrm{e}^{-2\alpha_0 T}(t - t_k)\sum_{j=0}^{m-1}\int_{x_j}^{x_{j+1}} w^\top w\mathrm{d}x\\
&\quad + 2\kappa\sum_{j=0}^{m-1}\int_{x_j}^{x_{j+1}} \big[q_1 \mathrm{e}^{-\mu x} R^\top(x,t) + q_2 \mathrm{e}^{\mu x} Q^\top(x,t)\big]\mathcal{D}\mathcal{L}_1\left[(t-t_k)w + \int_{\bar{x}_j}^{x} \epsilon_\xi(\xi,t_k)\mathrm{d}\xi\right]\mathrm{d}x\\
&\quad + \frac{\gamma}{4}(t_{k+1} - t)\sum_{j=0}^{m-1}\int_{x_j}^{x_{j+1}} \big[Q^\top(x,t) + R^\top(x,t)\big]\big[Q(x,t) + R(x,t)\big]\mathrm{d}x\\
&\quad - \kappa\sum_{j=0}^{m-1}\int_{x_j}^{x_{j+1}} \epsilon^\top(x,t)\mathcal{L}_1^\top\mathcal{L}_1\epsilon(x,t)\mathrm{d}x\\
&\quad - 2\alpha_1\sum_{j=0}^{m-1}\int_{x_j}^{x_{j+1}} \left[q_1 \mathrm{e}^{-\mu x} R^\top(x,t_k)R(x,t_k) + q_2 \mathrm{e}^{\mu x} Q^\top(x,t_k)Q(x,t_k)\right]\mathrm{d}x\\
&\quad + \frac{\kappa}{\pi^2}\sum_{j=0}^{m-1}\int_{x_j}^{x_{j+1}} \lambda_{\max}\big(\mathcal{L}_1^\top\mathcal{L}_1\big)\big[Q^\top(x,t) - R^\top(x,t)\big]\big[Q(x,t) - R(x,t)\big]\mathrm{d}x\\
&\quad + \frac{\tau_1}{4}\sum_{j=0}^{m-1}\int_{x_j}^{x_{j+1}} \big[Q(x,t_k) - R(x,t_k)\big]^\top\big[Q(x,t_k) - R(x,t_k)\big]\mathrm{d}x\\
&\quad - \tau_1\frac{\pi^2}{X^2}\sum_{j=0}^{m-1}\int_{x_j}^{x_{j+1}} \left[\int_{\bar{x}_j}^{x}\epsilon_\xi(\xi,t_k)\mathrm{d}\xi\right]^\top\left[\int_{\bar{x}_j}^{x}\epsilon_\xi(\xi,t_k)\mathrm{d}\xi\right]\mathrm{d}x. \qquad (19)
\end{aligned}$$

Define vectors

$$\begin{aligned}
Y_1 &= \left[\mathrm{e}^{-\mu x}R^\top(x,t),\ \mathrm{e}^{\mu x}Q^\top(x,t),\ w^\top,\ \int_{\bar{x}_j}^{x}\epsilon_\xi^\top(\xi,t_k)\mathrm{d}\xi,\ \epsilon^\top(x,t)\mathcal{L}_1^\top\right]^\top,\\
Y_2 &= \big[R^\top(x,t_k),\ Q^\top(x,t_k)\big]^\top. \qquad (20)
\end{aligned}$$

Then Eq. (19) can be rewritten in the following form:

$$\begin{aligned}
\dot{V}(t) + 2\alpha_0 V(t) - 2\alpha_1 \sup_{-T\leqslant\theta\leqslant 0} V(t+\theta) &\leqslant -q_1 \mathrm{e}^{-\mu} R^\top(1,t)R(1,t) - (q_2 - q_1)R^\top(0,t)R(0,t)\\
&\quad + \sum_{j=0}^{m-1}\int_{x_j}^{x_{j+1}} Y_1^\top(\Xi_1\otimes I_N)Y_1 + Y_2^\top(\Xi_2\otimes I_N)Y_2\mathrm{d}x, \qquad (21)
\end{aligned}$$

where

$$\Xi_2 \triangleq \begin{pmatrix} -2\alpha_1 q_1 \mathrm{e}^{-\mu x} + \frac{\tau_1}{2} & 0\\ 0 & -2\alpha_1 q_2 \mathrm{e}^{\mu x} + \frac{\tau_1}{2}\end{pmatrix}$$

and

$$\Xi_1 \triangleq \begin{pmatrix} \Xi_{11} & 0 & 0 & 0 & 0 \\ 0 & \Xi_{22} & 0 & 0 & 0 \\ 0 & 0 & \Xi_{33} & 0 & 0 \\ 0 & 0 & 0 & \Xi_{44} & 0 \\ 0 & 0 & 0 & 0 & -\kappa(1-q_1-q_2) \end{pmatrix}$$

with the diagonal elements being

$$\begin{aligned}
\Xi_{11} =& -(\mu-2\alpha_0)q_1\mathrm{e}^{\mu x}+2\kappa q_1+\kappa q_1(t-t_k)+\frac{\gamma}{2}(t_{k+1}-t)\mathrm{e}^{2\mu x}+\frac{2\kappa}{\pi^2}\lambda_{\max}\big(\mathcal{L}_1^\top\mathcal{L}_1\big)\mathrm{e}^{2\mu x},\\
\Xi_{22} =& -(\mu-2\alpha_0)q_2\mathrm{e}^{-\mu x}+2\kappa q_2+\kappa q_2(t-t_k)+\frac{\gamma}{2}(t_{k+1}-t)\mathrm{e}^{-2\mu x}+\frac{2\kappa}{\pi^2}\lambda_{\max}\big(\mathcal{L}_1^\top\mathcal{L}_1\big)\mathrm{e}^{-2\mu x},\\
\Xi_{33} =& -\gamma\mathrm{e}^{-2\alpha_0 T}(t-t_k)+\kappa(q_1+q_2)(t-t_k)\lambda_{\max}\big(\mathcal{L}_1^\top\mathcal{L}_1\big),\\
\Xi_{44} =& -\tau_1\frac{\pi^2}{X^2}+\kappa(q_1+q_2)\lambda_{\max}(\mathcal{L}_1^\top\mathcal{L}_1).
\end{aligned}$$

Let

$$\bar{\Xi}_{11} = -(\mu-2\alpha_0)q_1+2\kappa q_1+\kappa q_1\tau(t)+\frac{\gamma}{2}(T-\tau(t))\mathrm{e}^{2\mu}+\frac{2\kappa}{\pi^2}\lambda_{\max}\big(\mathcal{L}_1^\top\mathcal{L}_1\big)\mathrm{e}^{2\mu}, \tag{22}$$

$$\bar{\Xi}_{22} = -(\mu-2\alpha_0)q_2\mathrm{e}^{-\mu}+2\kappa q_2+\kappa q_2\tau(t)+\frac{\gamma}{2}(T-\tau(t))+\frac{2\kappa}{\pi^2}\lambda_{\max}\big(\mathcal{L}_1^\top\mathcal{L}_1\big), \tag{23}$$

$$\bar{\Xi}_{33} = -\gamma\mathrm{e}^{-2\alpha_0 T}\tau(t)+\kappa(q_1+q_2)\tau(t)\lambda_{\max}\big(\mathcal{L}_1^\top\mathcal{L}_1\big), \tag{24}$$

$$\bar{\Xi}_{44} = -\tau_1\frac{\pi^2}{X^2}+\kappa(q_1+q_2)\lambda_{\max}(\mathcal{L}_1^\top\mathcal{L}_1). \tag{25}$$

Then, by upper bounding the diagonal elements in the matrices Ξ_1 and Ξ_2, one has

$$\begin{aligned}
\Xi_1 \leqslant \bar{\Xi}_1 &\triangleq \begin{pmatrix} \bar{\Xi}_{11} & 0 & 0 & 0 & 0 \\ 0 & \bar{\Xi}_{22} & 0 & 0 & 0 \\ 0 & 0 & \bar{\Xi}_{33} & 0 & 0 \\ 0 & 0 & 0 & \bar{\Xi}_{44} & 0 \\ 0 & 0 & 0 & 0 & -\kappa(1-q_1-q_2) \end{pmatrix}, \\
\Xi_2 \leqslant \bar{\Xi}_2 &\triangleq \begin{pmatrix} -2\alpha_1 q_1\mathrm{e}^{-\mu}+\frac{\tau_1}{2} & 0 \\ 0 & -2\alpha_1 q_2+\frac{\tau_1}{2} \end{pmatrix}.
\end{aligned} \tag{26}$$

Note that Theorem 1 is verified once the matrices $\bar{\Xi}_1$ and $\bar{\Xi}_2$ are semi-negative definite and the following conditions hold simultaneously:

$$\begin{cases} 0 \leqslant q_2 - q_1, \\ 0 < \alpha_1 < \alpha_0 < \frac{1}{2}\mu. \end{cases}$$

Furthermore, for proper parameters $q_{1,2}$, μ, $\alpha_{0,1}$, and τ_1 satisfying inequalities (9) and (11), $\bar{\Xi}_2 \leqslant 0$ is easily obtained. Next, if Eq. (10) holds for sampling intervals in space $X > 0$ and time $T > 0$, the matrix $\bar{\Xi}_1$ is semi-negative definite by (12) and (26). Therefore, it derives

$$\dot{V}(t)+2\alpha_0 V(t)-2\alpha_1\sup_{-T\leqslant\theta\leqslant 0}V(t+\theta)\leqslant 0.$$

Finally, the conclusion is verified according to Lemma 1.

Remark 2. Other types of the Lyapunov-Krasovskii functional can be chosen. However, it may also increase computational complexity. In this paper, we choose the Lyapunov function $V_q(t)$ following the idea of [40], which can be viewed as the system energy. Furthermore, function $V_\gamma(t)$ is the simplest Lyapunov-Krasovskii term that treats sampled-data systems (see [42] for details).

Remark 3. The scalars q_1 and q_2 are introduced to make parameter selection more flexible. It is obvious from (10)–(12) that they will affect τ_1, γ, and control gain κ directly. In particular, formulas (22)–(25) imply that the control gain κ should not be so large that one can guarantee the bipartite containment control.

4 Well-posedness

In this section, the well-posedness of the PDE multi-agent system (1) with control protocol (2) is established. The induction method is used instead of the common techniques adopted by continuous-time systems due to the introduction of discrete sampled-data control law.

Some preliminary knowledge is necessary for clarifying the main result in this part. For brevity, we use the notation $L^2(0,1)$ for the standard space of square-integrable scalar functions defined on the interval $(0,1)$. The symbol $H^k(0,1)$ $(k=1,2)$ refers to the Sobolev space containing all the functions in $L^2(0,1)$ with all its weak derivatives up to order k also belonging to $L^2(0,1)$. Let $\mathcal{H}_0 = H_0^1(0,1)\times L^2(0,1)$ where $H_0^1(0,1)=\{f(\cdot)\in H^1(0,1)|f(0)=0\}$. The induced norm for any $(f,g)\in\mathcal{H}_0$ is

$$\|(f,g)\|_{\mathcal{H}_0} = \int_0^1 \left[|f'(x)|^2 + |g(x)|^2\right]\mathrm{d}x.$$

Furthermore, we employ $\mathcal{H}_0^{N+M}(0,1) = H_0^{1,N+M}(0,1)\times L^{2,N+M}(0,1)$, in which $H_0^{1,N+M}(0,1)$ and $L^{2,N+M}(0,1)$ are utilized for the Cartesian product of $N+M$ spaces $H_0^1(0,1)$ and $L^2(0,1)$, respectively. For any $(f,g)\in\mathcal{H}_0^{N+M}$, the corresponding norm is

$$\|(f,g)\|_{\mathcal{H}_0^{N+M}} = \sqrt{\sum_{i=1}^{N+M}\|(f_i,g_i)\|^2_{\mathcal{H}_0}}.$$

Theorem 2. For any initial values $(v_0(x),v_1(x))\in\mathcal{C}\big([0,+\infty),\mathcal{H}_0^{N+M}(0,1)\big)$, the closed-loop multi-agent system consisting of (1) and sampled-data control protocol (2) has a unique solution $(v(x,t),v_t(x,t))\in\mathcal{C}\big([0,+\infty),\mathcal{H}_0^{N+M}(0,1)\big)$.

Proof. Considering the control protocol (2), it is evident that the leader part is well-posed. As a result of the definition (3), the theorem can be established once the error system (4) contains a unique solution.

To this end, the error system (4) is represented as an abstract differential equation

$$\frac{\mathrm{d}}{\mathrm{d}t}(\epsilon_i(\cdot,t),\epsilon_{it}(\cdot,t)) = \boldsymbol{A}(\epsilon_i(\cdot,t),\epsilon_{it}(\cdot,t)) + (0,F_1(\epsilon_i,\cdot,t)) \tag{27}$$

with

$$\begin{aligned}F_1(\epsilon_i,\cdot,t) =& -\kappa\sum_{j=0}^{m-1}\chi_j(x)\sigma_i b_{ii}\left[\epsilon_i(\cdot,t_k) - \int_{\bar{x}_j}^{x}\epsilon_{i\xi}(\xi,t_k)\mathrm{d}\xi\right]\\ &+\kappa\sum_{j=0}^{m-1}\chi_j(x)\sum_{r=1,r\neq i}^{N}\sigma_i b_{ir}\int_{\bar{x}_j}^{x}\epsilon_{r\xi}(\xi,t_k)\mathrm{d}\xi - \kappa\sum_{j=0}^{m-1}\chi_j(x)\sum_{r=1,r\neq i}^{N}\sigma_i b_{ir}\epsilon_r(\cdot,t_k),\end{aligned}$$

where b_{ij}, $i,j\in\{1,\ldots,N\}$ are the elements in matrix $\mathcal{L}_1$, $t\in[t_k,t_{k+1}]$. Besides, the operator $\boldsymbol{A}$ has the following form:

$$\begin{cases}\boldsymbol{A}(f,g) = (g,f''), \quad \forall (f,g)\in D(\boldsymbol{A}),\\ D(\boldsymbol{A}) = \left\{\begin{array}{c|c}(f,g)\in & f(0)=0\\ H^2(0,1)\times H^1(0,1) & f'(1)=-g(1)\end{array}\right\}.\end{cases}$$

Simple calculations reveal that the operator $\boldsymbol{A}$ generates a C_0-semigroup of contractions via the Lumer-Phillips theorem [43].

First, let us focus on the initialization interval $[0,t_1]$ and prove that the unique solution of the closed-loop system belongs to a functional space. For interval $[0,t_1]$, it has

$$F_1(\epsilon_i,\cdot,t) = -\kappa\sum_{j=0}^{m-1}\chi_j(x)\sigma_i b_{ii}\left[\epsilon_i(\cdot,0) - \int_{\bar{x}_j}^{x}\epsilon_{i\xi}(\xi,0)\mathrm{d}\xi\right]$$

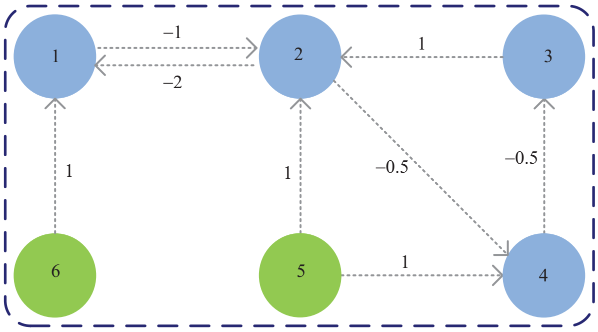

Figure 1 (Color online) Communication topology.

Table 1 Parameters for bipartite containment control

Name	Parameter value
Space sampling interval	$X = 0.1$
Time sampling interval	$T = 1$ s
Followers' initial values	$v_{10}(x) = \sin(2\pi x)$, $v_{11}(x) = 0.5x$ $v_{20}(x) = \sin(2\pi x + 1) - \sin(1)$, $v_{21}(x) = -x$ $v_{30}(x) = \sin(2\pi x + 2) - \sin(2)$, $v_{31}(x) = 2x$ $v_{40}(x) = \sin(2\pi x + 3) - \sin(3)$, $v_{41}(x) = 4x$
Leader's initial values	$v_{50}(x) = 1 - \cos(\pi x)$, $v_{51}(x) = \arctan(x)$ $v_{60}(x) = \cos(2\pi x) - 1$, $v_{61}(x) = \sin(\pi x)$
Control gain	$\kappa = 0.1 \times 10^{-3}$
Parameters in Halanay's inequality	$\alpha_0 = 0.5$, $\alpha_1 = 0.1$

$$- \kappa \sum_{j=0}^{m-1} \chi_j(x) \sum_{r=1,r\neq i}^{N} \sigma_i b_{ir} \epsilon_r(\cdot,0) + \kappa \sum_{j=0}^{m-1} \chi_j(x) \sum_{r=1,r\neq i}^{N} \sigma_i b_{ir} \int_{\bar{x}_j}^{x} \epsilon_{r\xi}(\xi,0)\mathrm{d}\xi.$$

The function F_1 is continuous in t and uniformly Lipschitz continuous with respect to ϵ_i. In terms of [43, Theorem 6.1.2], it can be seen that for any initial condition $(\epsilon_i(x,0), \epsilon_{it}(x,0)) \in \mathcal{H}_0(0,1)$, there exists a unique solution $(\epsilon_i(x,t), \epsilon_{it}(x,t)) \in \mathcal{C}\big([0,t_1], \mathcal{H}_0(0,1)\big)$.

In case that a unique trajectory $(\epsilon_i(x,t), \epsilon_{it}(x,t)) \in \mathcal{C}([t_k,t_{k+1}], \mathcal{H}_0(0,1))$ persists for system (27) on time interval $[t_k,t_{k+1}]$. Then, the initial state satisfies $(\epsilon_i(x,t_{k+1}), \epsilon_{it}(x,t_{k+1})) \in \mathcal{H}_0(0,1)$ over time interval $[t_{k+1},t_{k+2}]$, and one can find that

$$\begin{aligned} F_1(\epsilon_i,\cdot,t) = & - \kappa \sum_{j=0}^{m-1} \chi_j(x)\sigma_i b_{ii} \left[\epsilon_i(\cdot,t_{k+1}) - \int_{\bar{x}_j}^{x} \epsilon_{i\xi}(\xi,t_{k+1})\mathrm{d}\xi\right] \\ & - \kappa \sum_{j=0}^{m-1} \chi_j(x) \sum_{r=1,r\neq i}^{N} \sigma_i b_{ir} \left[\epsilon_r(\cdot,t_{k+1}) - \int_{\bar{x}_j}^{x} \epsilon_{r\xi}(\xi,t_{k+1})\mathrm{d}\xi\right]. \end{aligned}$$

Applying [43, Theorem 6.1.2], $(\epsilon_i(x,t), \epsilon_{it}(x,t)) \in \mathcal{C}\big([t_{k+1},t_{k+2}], \mathcal{H}_0(0,1)\big)$ is the unique solution of system (27) over time interval $t \in [t_{k+1},t_{k+2}]$.

By induction, for any natural number k, we can ensure the existence and uniqueness of solution $(\epsilon_i(x,t), \epsilon_{it}(x,t)) \in \mathcal{C}\big([0,+\infty), \mathcal{H}_0(0,1)\big)$ for error system (27). Therefore, the theorem is fulfilled on account of definition (3) and the leaders' dynamic equations.

5 Numerical simulations

This section discusses some numerical results that verify the effectiveness of the proposed control protocol. To proceed with the simulations clearly, the results are displayed at uniform sampling intervals, and the Chebyshev method is used.

Figure 1 is the communication topology, where the agents indexed by 5, 6 are leaders and others are followers. The followers can be divided into two opposing groups: $\mathcal{V}_1 = \{2,3\}$ and $\mathcal{V}_2 = \{1,4\}$.

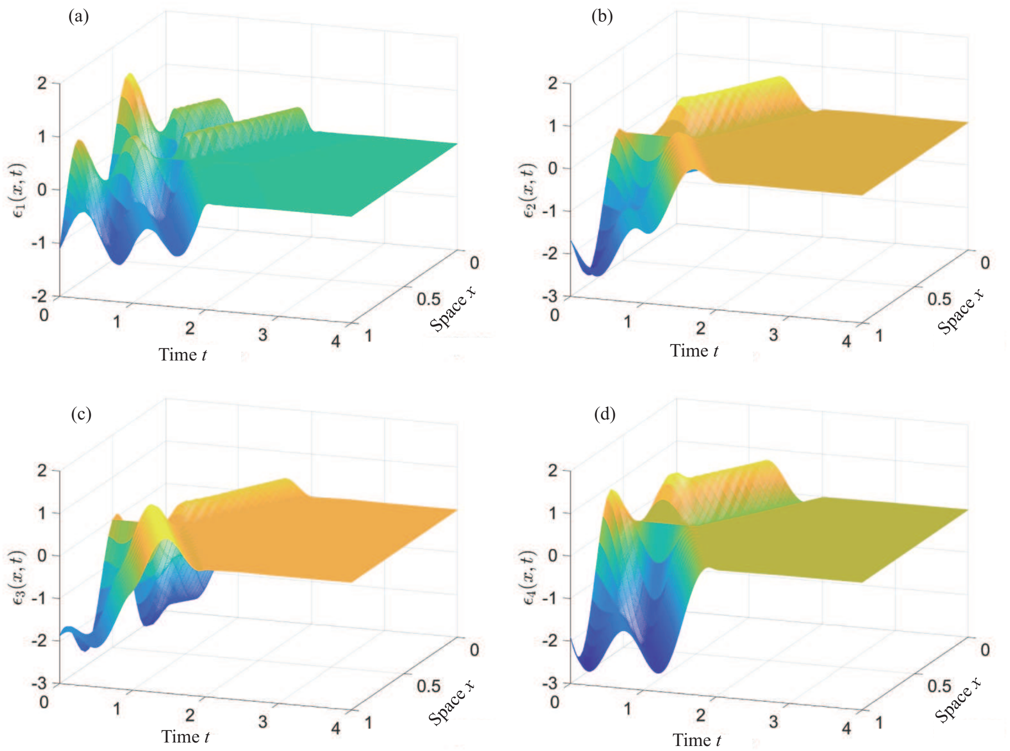

Figure 2 (Color online) Evolution of the components of error $\epsilon(x, t)$ over position x and time t. (a) $\epsilon_1(x, t)$; (b) $\epsilon_2(x, t)$; (c) $\epsilon_3(x, t)$; (d) $\epsilon_4(x, t)$.

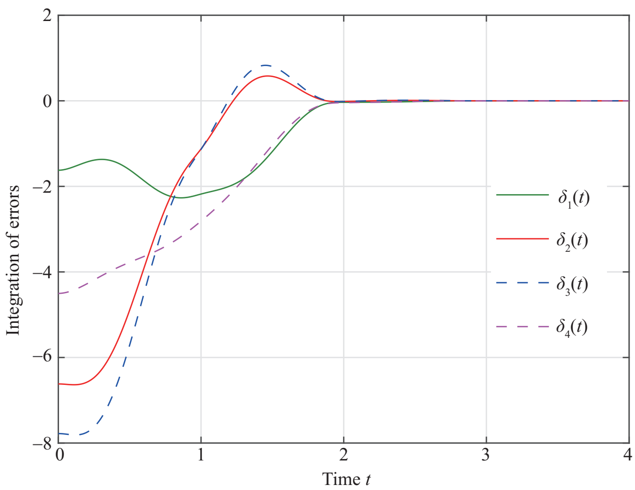

Figure 3 (Color online) Integration of error elements $\epsilon_i(x, t)$, $i \in \{1, \ldots, 4\}$.

Moreover, communication among agents in the same group is positive (friendly), and it becomes negative (unfavorable) for agents from different groups. Table 1 lists the parameters used in this simulation.

From Figure 2, the errors $\epsilon_i(x, t)$, $i \in \{1, \ldots, 4\}$ converge to zero eventually, which implies that bipartite containment control is guaranteed under the designed sampled-data protocol. Furthermore, to illustrate the results intuitively, Figure 3 exhibits the evolution of integration $\delta_i(t)$, $i \in \{1, \ldots, 4\}$ along with time t. Here, the notation $\delta_i(t)$ is defined by $\delta_i(t) = \int_0^1 \epsilon_i(x, t)\mathrm{d}x$. In terms of the simulation results, the proposed distributed sampled-data protocol renders the PDE followers into a convex hull spanned by leader states and their opposites. Thus, numerical simulations have verified the effectiveness of our proposed strategy.

6 Conclusion

In this paper, the infinite-dimensional bipartite containment control problem has been addressed. A sampled-data control protocol has been constructed to pursue the object. Subsequently, the well-posedness issue of the closed-loop system was discussed via the semigroup and induction approach. Finally, numerical simulations are provided to support our theoretical findings.

Acknowledgements This work was supported by National Natural Science Foundation of China (Grant Nos. 62173243, 61933014, 62203327).

References

1 Olfati-Saber R, Fax J A, Murray R M. Consensus and cooperation in networked multi-agent systems. Proc IEEE, 2007, 95: 215–233
2 Yu W, Ren W, Zheng W X, et al. Distributed control gains design for consensus in multi-agent systems with second-order nonlinear dynamics. Automatica, 2013, 49: 2107–2115
3 Zhang Y, Liu Y, Yang X, et al. A reset algorithm solving coordination with antagonistic reciprocity. IEEE Trans Syst Man Cybern Syst, 2022, 52: 2361–2371
4 Liu K, Ji Z. Dynamic event-triggered consensus of general linear multi-agent systems with adaptive strategy. IEEE Trans Circuits Syst II, 2022, 69: 3440–3444
5 Ji M, Ferrari-Trecate G, Egerstedt M, et al. Containment control in mobile networks. IEEE Trans Automat Contr, 2008, 53: 1972–1975
6 Shan Q H, Teng F, Li T S, et al. Containment control of multi-agent systems with nonvanishing disturbance via topology reconfiguration. Sci China Inf Sci, 2021, 64: 179203
7 Cao Y, Ren W, Egerstedt M. Distributed containment control with multiple stationary or dynamic leaders in fixed and switching directed networks. Automatica, 2012, 48: 1586–1597
8 Li Z, Ren W, Liu X, et al. Distributed containment control of multi-agent systems with general linear dynamics in the presence of multiple leaders. Int J Robust Nonlinear Control, 2013, 23: 534–547
9 Wang Y, Cheng L, Hou Z G, et al. Containment control of multi-agent systems in a noisy communication environment. Automatica, 2014, 50: 1922–1928
10 Altafini C. Consensus problems on networks with antagonistic interactions. IEEE Trans Automat Contr, 2013, 58: 935–946
11 Meng D. Bipartite containment tracking of signed networks. Automatica, 2017, 79: 282–289
12 Liu J, He W. Distributed Parameter Modeling and Boundary Control of Flexible Manipulators. Singapore: Springer, 2018
13 Chen T, Wen H, Wei Z. Distributed attitude tracking for multiple flexible spacecraft described by partial differential equations. Acta Astronaut, 2019, 159: 637–645
14 Demetriou M A. Synchronization and consensus controllers for a class of parabolic distributed parameter systems. Syst Control Lett, 2013, 62: 70–76
15 Pilloni A, Pisano A, Orlov Y, et al. Consensus-based control for a network of diffusion PDEs with boundary local interaction. IEEE Trans Automat Contr, 2016, 61: 2708–2713
16 Deutscher J. Cooperative output regulation for a network of parabolic systems with varying parameters. Automatica, 2021, 125: 109446
17 Deutscher J. Robust cooperative output regulation for a network of parabolic PDE systems. IEEE Trans Automat Contr, 2022, 67: 451–459
18 Aguilar L, Orlov Y, Pisano A. Leader-follower synchronization and ISS analysis for a network of boundary-controlled wave PDEs. IEEE Control Syst Lett, 2021, 5: 683–688
19 Chen Z Z, Yang J, Zong X. Leader-follower synchronization controller design for a network of boundary-controlled wave PDEs with structured time-varying perturbations and general disturbances. J Franklin Institute, 2021, 358: 834–855
20 Chen Y, Zuo Z, Wang Y. Bipartite consensus for a network of wave equations with time-varying disturbances. Syst Control Lett, 2020, 136: 104604
21 Chen Y, Zuo Z, Wang Y. Bipartite consensus for a network of wave PDEs over a signed directed graph. Automatica, 2021, 129: 109640
22 Chen Y, Zuo Z, Wang Y. Scaled consensus over a network of wave equations. IEEE Trans Control Netw Syst, 2022, 9: 1385–1396
23 Demetriou M A. Design of adaptive output feedback synchronizing controllers for networked PDEs with boundary and in-domain structured perturbations and disturbances. Automatica, 2018, 90: 220–229
24 Singh V K, Natarajan V. Finite-dimensional controllers for consensus in a leader-follower network of marginally unstable infinite-dimensional agents. IEEE Control Syst Lett, 2022, 6: 590–595
25 Wei J Q, Fridman E, Johansson K H. A PDE approach to deployment of mobile agents under leader relative position measurements. Automatica, 2019, 106: 47–53
26 Terushkin M, Fridman E. Network-based deployment of nonlinear multi agents over open curves: a PDE approach. Automatica, 2021, 129: 109697
27 Freudenthaler G, Meurer T. PDE-based multi-agent formation control using flatness and backstepping: analysis, design and robot experiments. Automatica, 2020, 115: 108897
28 Fridman E, Seuret A, Richard J P. Robust sampled-data stabilization of linear systems: an input delay approach. Automatica, 2004, 40: 1441–1446
29 Karafyllis I, Krstic M. Nonlinear stabilization under sampled and delayed measurements, and with inputs subject to delay and zero-order hold. IEEE Trans Automat Contr, 2012, 57: 1141–1154
30 Wu X H, Mu X W. Novel dynamic event-triggered coordination for scaled consensus without continuous communication or controller update. Sci China Inf Sci, 2022, 65: 209202
31 Wang J W, Tsai S H, Li H X, et al. Spatially piecewise fuzzy control design for sampled-data exponential stabilization of semilinear parabolic PDE systems. IEEE Trans Fuzzy Syst, 2018, 26: 2967–2980
32 Fridman E, Blighovsky A. Robust sampled-data control of a class of semilinear parabolic systems. Automatica, 2012, 48: 826–836

33 Karafyllis I, Krstic M. Sampled-data boundary feedback control of 1-D parabolic PDEs. Automatica, 2018, 87: 226–237
34 Karafyllis I, Krstic M. Sampled-data boundary feedback control of 1-D linear transport PDEs with non-local terms. Syst Control Lett, 2017, 107: 68–75
35 Davo M A, Bresch-Pietri D, Prieur C, et al. Stability analysis of a 2×2 linear hyperbolic system with a sampled-data controller via backstepping method and looped-functionals. IEEE Trans Automat Contr, 2019, 64: 1718–1725
36 Logemann H, Rebarber R, Townley S. Generalized sampled-data stabilization of well-posed linear infinite-dimensional systems. SIAM J Control Optim, 2016, 44: 1345–1369
37 Rebarber R, Townley S. Robustness with respect to sampling for stabilization of riesz spectral systems. IEEE Trans Automat Contr, 2006, 51: 1519–1522
38 Gockenbach M S. Partial Differential Equations: Analytical and Numerical Methods. Philadelphia: SIAM, 2011
39 Halanay A. Differential Equations: Stability, Oscillations, Time Lags. New York: Academic Press, 1966
40 Bastin G, Coron J-M. Stability and Boundary Stabilization of 1-D Hyperbolic Systems. Berlin: Springer, 2016
41 Hardy G H, Littlewood J E, Polya G. Inequalities. Cambridge: Cambridge University Press, 1934
42 Fridman E. A refined input delay approach to sampled-data control. Automatica, 2010, 46: 421–427
43 Pazy A. Semigroups of Linear Operators and Applications to Partial Differential Equations. New York: Springer-Verlag, 1983